中國機械工程學刊第四十二卷第五期第 509~519 頁(民國一百一十年)
Journal of the Chinese Society of Mechanical Engineers, Vol.42, No.5, pp. 509~519 (2021)

Tooth Flank Modification of a Helical Gear by Using Modified Tangential Dressing Motion in a Gear Generating Grinding Machine

Gwan-Hon Chen** and Zhang-Hua Fong*

Keywords：tangential dressing motion, generating grinding, helical gear, tooth flank modification.

ABSTRACT

The tooth flank of a ground helical gear is conventionally crowned by adjusting the radial feed of the grinding worm while the grinding worm is moving axially with respect to the working gear in a modern computer numerical control (CNC) gear generating grinding machine. However, the tooth flank of a helical gear crowned using this modified radial feed method is frequently twisted. Therefore, we propose a tooth flank modification method for helical gears with the grinding worm fed diagonally (combined tangential and axial feed) while the grinding worm is meshing with the working gear in a grinding machine. In addition, the grinding worm is dressed by the dressing disk with additional tangential dressing motion (TDM) while the dressing disk is moving axially with respect to the rotating grinding worm. Because all the required corrective motions for the proposed TDM method are existing CNC controlled axes in modern gear grinding machines, the proposed method can be implemented easily without modifying the grinder hardware. Two numerical examples are presented to validate the proposed TDM tooth flank modification method with four simultaneously controlled axes

INTRODUCTION

Involute helical gears generated by a grinding worm in a generating grinding machine are widely used in industry for high productivity. However, a twisted tooth flank results when the tooth crowning for a helical gear is manufactured using such a modification, several methods have been proposed that involve using five-axis motion flexibility of a computer numerical control (CNC) grinding machine. However, the anti-twist effect is limited by modifying the CNC corrective motions only if the geometry of the grinding worm is maintained similarly to that of a standard worm surface. Therefore, we propose a tooth flank modification method for grinding helical gears that entails using an existing generating grinding machine without additional effort or costs to modify the grinder hardware.

Litvin, Zhang, and Handschuh (1988) proposed a generation process with a five degree of freedom (DOF) mechanism for modifying the tooth flanks of involute gears to prevent gear edge contact and reduce transmission errors. Bouzakis (1995) proposed a methodology for optimizing the tangential tool shift in gear hobbing. The helical gear tooth geometry and basic meshing equations are derived from Litvin (2004) and Dudley (2011). Karpuschewski et al. (2008) illustrated a finishing tool and dressing motion by detailing a gear finishing tooth surface and working process. The bias error of helical gear tooth flanks caused by radial feed adjustment cutting methods was aptly explained by Lange (2009), who also proposed a methodology for optimizing it according to contact behavior. Xu et al. (2009) illustrated the effects of axis deflection and bias errors on a tooth surface and the stress distributions of a hypoid gear.

Chen et al. (2009) employed a mathematical model to simulate a gear hobbing process with two DOFs. To further support the application of gear hobbing and grinding machines, Siemens researchers (2012) developed a specialized function—an electronic gear box bundled into their CNC controller—to reduce the effort of CNC programing for hobbing processes. Fan et al. (2008) proposed flank correction methodologies based on the CNC hypoid gear generator. Winkel (2010) developed a hobbing process for crowned gears with a diagonal feed that reduced tooth flank twist in the workpiece.

Shih and Chen (2012) have proposed a tooth flank modification grinding method with a high-order correction based on a five-axis CNC gear profile grinding machine for reducing tooth flank twist. Hsu et al. (2014) have proposed a modified hob with

Paper Received May, 2016. Revised September, 2017. Accepted October, 2017. Author for Correspondence: Zhang-Hua Fong

* *Professor, Department of Mechanical Engineering, National Chung Cheng University, Chiayi, Taiwan 621301, ROC.*

** *Graduate Student, Department of Mechanical Engineering, National Chung Cheng University, Chiayi, Taiwan 621301, ROC.*

variable tooth thickness for reducing tooth flank twist in longitudinal crowning. Tran et al. (2014) proposed a low-twist hobbing process with its tangential feed as a second-order function of axial movement that involves using a dual-lead hob cutter with a pressure angle change. Jiang and Fang (2015) used six-axis high-order tooth flank corrective motion in a CNC hobbing machine by employing sensitivity analysis to reduce tooth flank twist.

In this paper, we propose a tooth flank modification method for helical gears with a grinding worm fed diagonally (combined tangential and axial feed) while the grinding worm is meshing with the working gear in a grinding machine. The grinding worm is dressed by the dressing disk with additional tangential dressing motion (TDM) while the dressing disk is moving axially with respect to the rotating grinding worm. With such four CNC axis corrective motions and the modified TDM grinding worm, the twist of a modified tooth flank can be reduced to a negligible level. Because all the required corrective motions for the proposed TDM method are the existing CNC controlled axes in a modern gear grinder, it can be implemented easily without additional cost to modify the gear grinder hardware. Three numerical examples are presented to validate the proposed TDM tooth flank modification method with four simultaneously controlled axes

.MATHEMATICAL MODEL OF DRESSING A WORM GRINDING WHEEL

As shown in Figure 1, a generating grind machine for helical gears typically has six CNC controlled axes: three linear and three rotational movements. The axial feed Z is parallel to the workpiece rotation axis C. Moreover, the tangential feed X moves along the rotation axis of the grinding worm B. The radial feed Y is perpendicular to the workpiece axis C and along the infeed axis of the moving column. The workpiece rotates about axis C. The cross angle A is the angle between the grinding worm axis and workpiece rotation axis C. The grinding worm rotates about axis B, and the dressing disk rotates about axis V. In a typical gear grinding factory, the dressing disk is purchased from machine tool suppliers. The profile of a dressing disk, which is defined at the design stage, is generally custom-made. The grinding worm profile is shaped by a dressing disk through a form dressing process, and the working gear profile is generated by the grinding worm through a generating grinding process. If the tooth flank modification method for generating grinding were developed using the six existing CNC axes or their subsets, the developed tooth flank modification could be implemented through CNC programing without changing any hardware of the grinding machine.

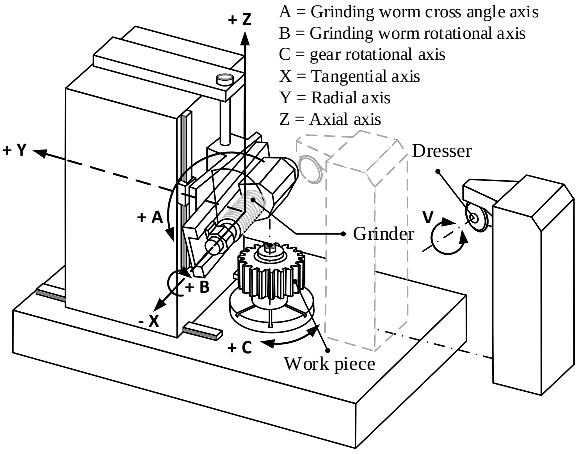

Fig. 1 Definition of axes in a gear grinding machine

The grinding worm is dressed by a rotating dressing disk mounted on the V axis, as shown in Fig. 1. The dressing process requires five DOFs and the X, Y, Z, V, B, and A axes in the grinder. In the conventional dressing process, the grinding worm is a thread of a constant pitch. The grinding worm rotates and moves axially at constant speeds; that is, two simultaneously controlled axes, B and X, are required in the conventional dressing process. The other four axes—Y, Z, V, and A—are the machine settings that are maintained constant during the dressing process.

However, in the proposed tooth flank modification method, the grinding worm is dressed with three simultaneously controlled axes, B, X, and Z, whereas the other three axes, Y, A, and V, are the machine settings. The movement Z provides an additional tangential shift with respect to the grinding worm. The coordinate systems for the grinding worm dressing process are shown in Fig. 2, in which coordinate systems $S_w(x_w, y_w, z_w)$ and $S_d(x_d, y_d, z_d)$ are rigidly connected to the grinding worm and dresser, respectively.

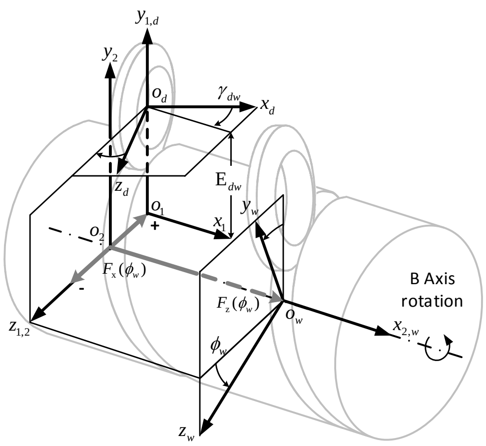

Fig. 2 Coordinate system of the schematic generation mechanism for grinding worm dressing

The coordinate system $S_2(x_2, y_2, z_2)$ is the auxiliary coordinate system for the dressing feed. A CNC gear grinding machine involves three grinding worm movements: a traverse movement $F_x(\phi_w)$ along the axis of the grinding worm (the X axis movement), a tangential movement $F_z(\phi_w)$ along the axis of gear (the Z axis movement), and a rotary motion, the rotation of the grinding worm ϕ_w (the B axis motion). Because the dresser is circular, the dressing disk rotation angle can be disregarded in deriving mathematical formulas.

The profile used to polynomial grinding worm that is generated by the dressing disk. The profile of the dressing disk is shown in Fig. 3.

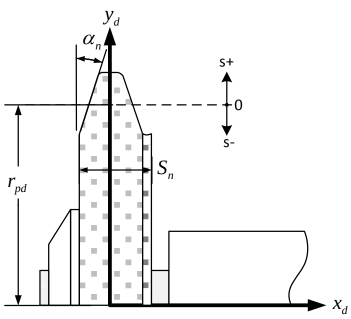

Fig. 3 Coordinate system of the dressing disk profile

This latter is combined with profile modification $F_p(s)$, as expressed in Equation (4) in polynomial form, to produce the dressing disk's actual normal profile $\mathbf{\Gamma}_d(s)$. The surface position vector $\mathbf{\Sigma}_d$, the dressing disk's normal vector $\mathbf{N}_d$, and its actual normal profile $\mathbf{\Gamma}_d(s)$ can then be expressed as:

$$\mathbf{\Sigma}_d(\theta,s)=\begin{bmatrix}\mathbf{\Sigma}_{dx} & \mathbf{\Sigma}_{dy} & \mathbf{\Sigma}_{dz} & 1\end{bmatrix}^T=\mathbf{M}_d\,\mathbf{\Gamma}_d$$

(1) (1)

$$\mathbf{N}_d(\theta,s)=\begin{bmatrix}N_{dx} & N_{dy} & N_{dz}\end{bmatrix}^T=\frac{\partial\mathbf{\Sigma}_d(\theta,s)}{\partial\theta}\times\frac{\partial\mathbf{\Sigma}_d(\theta,s)}{\partial s} \quad (2)$$

$$\mathbf{\Gamma}_d(s)=\begin{bmatrix}x_d(s)\mp F_p(s) & s+r_{pd} & 0 & 1\end{bmatrix}^T$$

(3) (3)

where

$$\mathbf{M}_d=\begin{bmatrix}1 & 0 & 0 & 0\\ 0 & \cos\theta & -\sin\theta & 0\\ 0 & \sin\theta & \cos\theta & 0\\ 0 & 0 & 0 & 1\end{bmatrix}$$

$$F_p(s)=v_1\left(\frac{s}{m}\right)+v_2\left(\frac{s}{m}\right)^2+v_3\left(\frac{s}{m}\right)^3 \quad (4)$$

(4)

where $\mp$ indicates the right or left profile of the dressing disk, r_{pd} is the pitch radius of the dressing disk, and m and m_n are the module and normal module, respectively. The profile function $x_d(s)$ is expressed as follows:

$$x_d(s)=\pm\frac{S_n}{2}\mp s\tan\alpha_n$$

(5)

where $S_n=m_n\,\pi/2$, And α_n is the pressure angle, S_n is the tooth thickness, and $\pm$ and $\mp$ indicate the right or left profile of the dressing disk.

The profile modification of dressing disk $F_p(s)$ is simplified as a third-order polynomial of a parameter. The degree of the polynomial is subject to change depending on the accuracy requirement. When a higher DOF is required for specific tooth profile modifications, a piecewise polynomial curve such as a cubic spline can be used. The modification effect on the dressing disk's normal profile in terms of polynomial coefficients is outlined in Table 1, in which coefficients v_1-v_3 are the design parameters to be used in tooth surface topology optimization.

Table 1 Modification effect on the dressing disk profile in terms of polynomial coefficients

Coefficient	Schematic diagram	Modification Type
$\boldsymbol{v_1}$	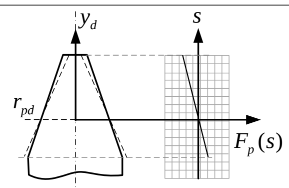	Pressure angle
$\boldsymbol{v_2}$	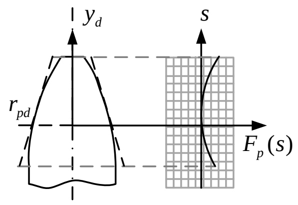	Profile crowning
$\boldsymbol{v_3}$	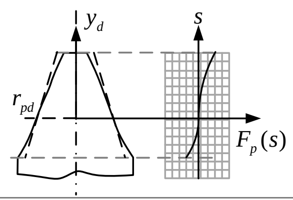	Inflection profile

As shown in Fig. 2, the tangential dressing is formed by the dressing disk moving at axial feed $F_z(\phi_w)$ as the grinding worm rotates at constant speed. The grinding worm tooth surface Σ_w is derived as follows:

$$\mathbf{r}_w=\begin{bmatrix}r_{wx} & r_{wy} & r_{wz} & 1\end{bmatrix}^T=\mathbf{M}_{wd}\,\mathbf{\Sigma}_d$$

(6) (5)

$$\mathbf{n}_w=\begin{bmatrix}n_{wx} & n_{wy} & n_{wz}\end{bmatrix}^T=\mathbf{L}_{wd}\,\mathbf{N}_d$$

(7) (6)

$$\boldsymbol{\Sigma}_w = \begin{cases} \mathbf{r}_w(s,\theta,\phi_w) \\ f_{\phi_w}(s,\theta,\phi_w) = \mathbf{n}_w \cdot \dfrac{\partial \mathbf{r}_w}{\partial \phi_w} = 0 \end{cases}$$

(8) (7)

where

$$\mathbf{M}_{wd} = \mathbf{M}_{w2}\,\mathbf{M}_{21}\,\mathbf{M}_{1d} = \begin{bmatrix} 1 & 0 & 0 & F_x(\phi_w) \\ 0 & \cos\phi_w & \sin\phi_w & 0 \\ 0 & -\sin\phi_w & \cos\phi_w & 0 \\ 0 & 0 & 0 & 1 \end{bmatrix} \begin{bmatrix} 1 & 0 & 0 & 0 \\ 0 & 1 & 0 & 0 \\ 0 & 0 & 1 & F_z(\phi_w) \\ 0 & 0 & 0 & 1 \end{bmatrix} \begin{bmatrix} \cos\gamma_{dw} & 0 & -\sin\gamma_{dw} & 0 \\ 0 & 1 & 0 & -E_{dw} \\ \sin\gamma_{dw} & 0 & \cos\gamma_{dw} & 0 \\ 0 & 0 & 0 & 1 \end{bmatrix}$$

$$F_x(\phi_w) = \pm P_w\,\phi_w \tag{9}$$

(8)

$$F_z(\phi_w) = v_4\left(\frac{2P_w\phi_w}{b_w}\right)^2 + v_5\left(\frac{2P_w\phi_w}{b_w}\right)^3 \tag{10}$$

(9)

Here, $\mathbf{L}_{wd}$ is the upper left (3×3) submatrix of $\mathbf{M}_{wd}$, and the crossed angle γ_{dw} and operating center distance E_{dw} between the grinding worm and dressing disk axes correspond to machine settings.

As Eq. (10) shows, the tangential feed of the grinding worm $F_z(\phi_w)$ is simplified as a second- and third-order polynomial. Parameter P_w is the screw parameter of the grinding worm.

Again, the degree of the polynomial is subject to change depending on the accuracy requirement, and a piecewise polynomial curve such as a cubic spline can be used when a specific modification requires a higher DOF.The modification effect on the grinding worm in terms of polynomial coefficients is illustrated in Fig. 4, where the coefficients v_4 and v_5 are the design parameters to be used in tooth surface topology optimization. The term b_w represents the working length of the grinding worm, and b_w is a constant value in the dressing process.

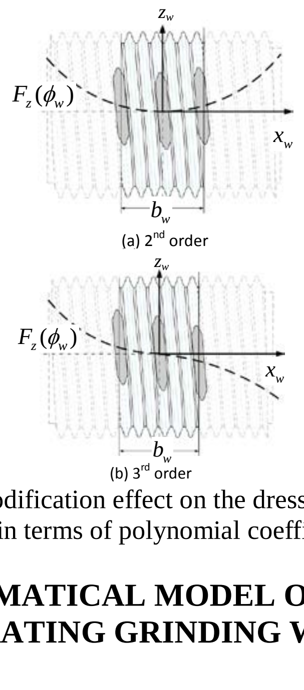

Fig. 4 Modification effect on the dressing disk profile in terms of polynomial coefficients

MATHEMATICAL MODEL OF GEAR GENERATING GRINDING WITH A WORM GRINDING WHEEL

The CNC axes in a gear grinding machine and the corresponding coordinate systems for gear generating grinding are shown in Fig. 1. The motion control diagram for the gear grinding machine is shown in Fig. 5, in which the gear set icon defines a constant gear ratio applied to fulfill a specific relative motion between the working gear and grinding worm in a standard gear generating process. The curved table icon represents a modified function added to the corresponding standard constant gear ratio to modify the working gear's tooth surface topology. The bold line indicates the proposed four-axis machining in this simulation.

As Fig. 6 shows, coordinate systems $S_w$andS_g are rigidly connected to the grinding worm and working gear, respectively, and coordinate systems S_3 , S_4 , and S_5 , respectively, are the auxiliary coordinate systems defining the grinding worm's tangential, radial, and axial feeds during the gear grinding process. The grinding worm has three movements: axial feed z along the axis of gear z_g, tangential feed F_T along the axis of grinding worm x_3 , and radial feed F_R along the center distance between the grinding worm and the working gear (the Z, X, and Y axes in Fig. 1). It also has two rotary motions: that of the working gear and that of the grinding worm (the C and B axis rotations in Fig. 1).

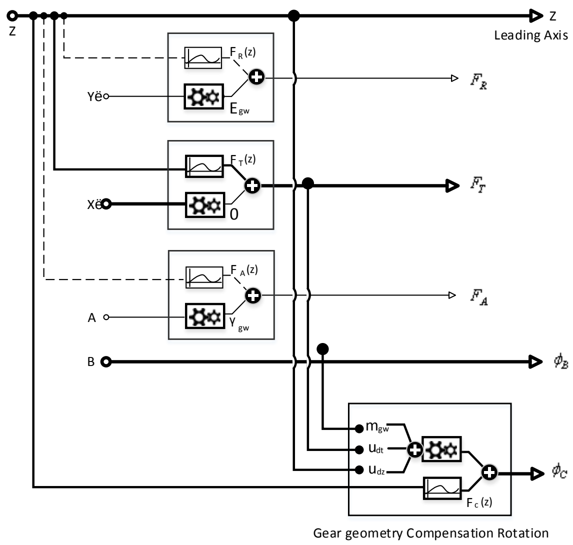

Fig. 5 Electronic gear box of a CNC gear grinding machine controller

$$\mathbf{r}_g = \begin{bmatrix} r_{gx} & r_{gy} & r_{gz} & 1 \end{bmatrix}^T = \mathbf{M}_{gw}\,\mathbf{r}_w$$

(11) (10)

$$\mathbf{n}_g = \begin{bmatrix} n_{gx} & n_{gy} & n_{gz} \end{bmatrix}^T = \mathbf{L}_{gw}\,\mathbf{n}_w$$

(12) (11)

$$\begin{cases} \mathbf{r}_g(s,\theta,\phi_w,\phi_B,z) \\ f_{\phi_B}(s,\theta,\phi_w,\phi_B,z) = \mathbf{n}_g(s,\theta,\phi_w,\phi_B,z)\cdot\dfrac{\partial \mathbf{r}_g(s,\theta,\phi_w,\phi_B,z)}{\partial \phi_B} = 0 \\ f_z(s,\theta,\phi_w,\phi_B,z) = \mathbf{n}_g(s,\theta,\phi_w,\phi_B,z)\cdot\dfrac{\partial \mathbf{r}_g(s,\theta,\phi_w,\phi_B,z)}{\partial z} = 0 \\ f_{\phi w}(s,\theta,\phi w) = 0 \end{cases} \tag{13}$$

where

$$\mathbf{M}_{gw} = \mathbf{M}_{g3}\mathbf{M}_{31}\mathbf{M}_{1w}$$

$$\mathbf{M}_{1w} = \begin{bmatrix} 1 & 0 & 0 & F_T(z) \\ 0 & \cos\phi_B & -\sin\phi_B & 0 \\ 0 & \sin\phi_B & \cos\phi_B & 0 \\ 0 & 0 & 0 & 1 \end{bmatrix}$$

$$\mathbf{M}_{g1} = \mathbf{M}_{g3}\mathbf{M}_{31}$$

$$\mathbf{M}_{g3} = \begin{bmatrix} \cos\phi_C(\phi_B,z) & -\sin\phi_C(\phi_B,z) & 0 & 0 \\ \sin\phi_C(\phi_B,z) & \cos\phi_C(\phi_B,z) & 0 & 0 \\ 0 & 0 & 1 & 0 \\ 0 & 0 & 0 & 1 \end{bmatrix}$$

$$\mathbf{M}_{31} = \begin{bmatrix} \cos\phi_A & 0 & \sin\phi_A & 0 \\ 0 & 1 & 0 & F_R \\ -\sin\phi_A & 0 & \cos\phi_A & z \\ 0 & 0 & 0 & 1 \end{bmatrix}$$

$$m_{wg} = \frac{z_w}{z_g}$$

$$F_T(z) = \pm\frac{b_w}{b_g} z \tag{14}$$

where $\pm$ indicates the same or opposite rotational direction of the grinding worm and working gear.

$$\phi_A = \gamma_{gw} + \frac{1}{2\pi\, m_n} v_6$$
$$\gamma_{gw} = -(\beta_g \mp \lambda_w) \tag{15}$$

where $\mp$ indicates the same or opposite rotational direction of the grinding worm and working gear. The terms β_g and λ_w denote the helical angle of the working gear and the lead angle of the grinding worm, respectively.

$$F_R = E_{gw} + \frac{1}{\tan\alpha_n} v_7 \tag{16}$$

$$E_{gw} = r_{pg} + r_{pw} + x_{ng} \tag{17}$$

where r_{pg} and r_{pw} denote the pitch radius of the working gear and grinding worm, respectively, and x_{ng} is the profile shift of the workpiece.

$$\phi_C(\phi_B, z) = F_C(z) + m_{wg}\ \phi_B + m_{wg}\ u_{dT}\ F_T(z) + u_{dz}\ z \tag{18}$$

$$F_C(z) = \frac{1}{r_{og}}\left(v_8 \left(\frac{2}{b_g} z\right)^2 + v_9 \left(\frac{2}{b_g} z\right)^3 \right) \tag{19}$$

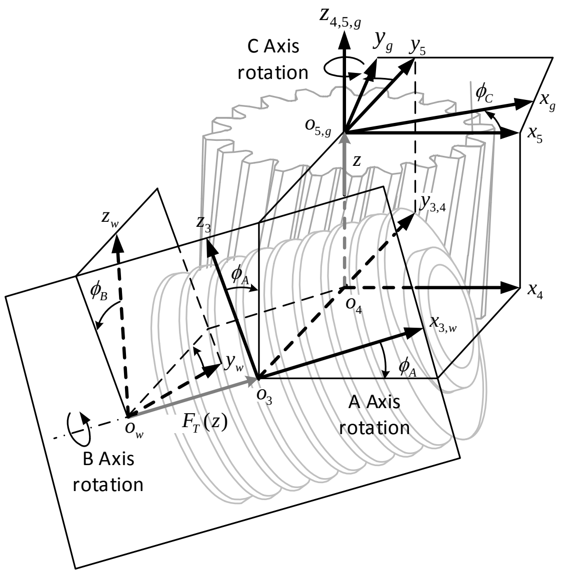

Fig. 6 Coordinate system of the schematic generation mechanism for gear grinding

SURFACE NORMAL DEVIATION TOPOGRAPHY OF THE WORKPIECE AND SENSITIVITY MATRIX

Tooth surface normal deviation topography is commonly used to depict the effect of tooth surface modification. First, the working gear tooth surface is digitized as a grid mesh with a varied transverse section (Z_i) in the lead direction and a varied radius (R_i) in the profile direction (Fig. 7). The normal deviation of the tooth flank can then be calculated at the grid points with specified (Z_i, R_i) by comparing the modified tooth flank surface $\mathbf{\Sigma}_g$ of the working gear with the standard working gear surface $\mathbf{\Sigma}_g{}'$. The normal deviations m_i of the working gear and standard gear tooth surfaces at grid points can be obtained by solving the following simultaneous system of equations:

$$\begin{cases} m_i = \mathbf{N}_g \cdot (\mathbf{\Sigma}_g - \mathbf{\Sigma}'_g) \\ \mathbf{\Sigma}_{gx}{}^2 + \mathbf{\Sigma}_{gy}{}^2 = R_i^2 \quad , \quad i = 1,2,....,p \\ \mathbf{\Sigma}_{gz} = Z_i \end{cases}$$

(20) (19)

As illustrated in Fig. 7, the standard working gear surface, drawn as a flat grid mesh of thin black lines, is the datum for comparison with the modified tooth surface, which is drawn in thick red lines. The total number p of mesh grid points is $p = 5 \times 5 = 25$, with a 5 x 5 mesh on each of the two surface sides shown. The outward normal deviation indicates that the modified tooth surface is thicker than the standard tooth surface, whereas the normal deviation topography reveals the differences between the work piece and standard gear tooth surfaces. The mesh grid points can be expressed as follows, where r_m is the center of the tooth profile and can be defined as $0.5(r_s + r_e)$. The terms r_s and r_e are respectively the start and end of the active profile.

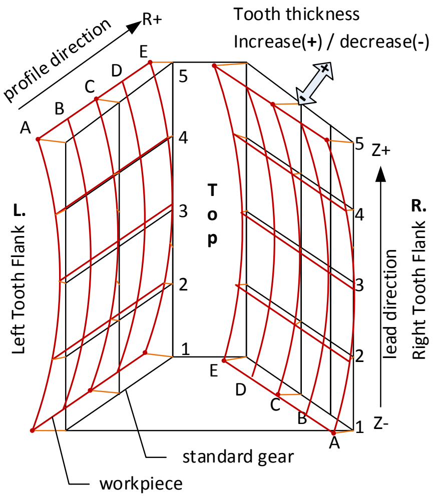

Fig. 7 Normal deviation topography for the 5×5 mesh grid points on tooth surface

We now require a methodology for determining the design variables ($\upsilon_1 - \upsilon_9$) for the tooth surface modification that optimally approximates the desired tooth surface topology. The most common methods for deriving such variables are singular value decomposition (SVD) and least squares error estimation (LSE) with a weight method, although a sensitivity matrix is also required for surface approximation. Because the sensitivity matrix M_S is the first partial differentiation of the surface normal deviation m_i with respect to design variables υ_j, a change in the normal deviation δm_i at the ith point is a linear combination of the normal deviation change resulting from varied change δv_j in the design variables. Hence, the desired normal deviation topography is given (i.e., $\{\delta m_i\}$ is known):

$$\{\delta m_i\} = \mathbf{M}_S \{\delta \upsilon_j\} = [\frac{\partial m_i}{\partial \upsilon_j}]\{\delta \upsilon_j\} \qquad (21)$$

$$(i = 1, 2..., p;\ j = 1, 2..., 9)$$

where

$$M_S = \begin{bmatrix} \delta m_1 \\ \delta m_2 \\ \vdots \\ \delta m_{24} \\ \delta m_{25} \end{bmatrix};$$

$$= \begin{bmatrix} w_1 \partial m_1/\partial \upsilon_1 & w_2 \partial m_2/\partial \upsilon_1 & \dots & w_{24} \partial m_{24}/\partial \upsilon_1 & w_{25} \partial m_{25}/\partial \upsilon_1 \\ w_1 \partial m_1/\partial \upsilon_3 & w_2 \partial m_2/\partial \upsilon_2 & \dots & w_{24} \partial m_{24}/\partial \upsilon_2 & w_{25} \partial m_{25}/\partial \upsilon_2 \\ \vdots & \vdots & \vdots & \vdots & \vdots \\ w_1 \partial m_1/\partial \upsilon_8 & w_2 \partial m_2/\partial \upsilon_8 & \dots & w_{24} \partial m_{24}/\partial \upsilon_8 & w_{25} \partial m_{25}/\partial \upsilon_8 \\ w_1 \partial m_1/\partial \upsilon_9 & w_2 \partial m_2/\partial \upsilon_9 & \dots & w_{24} \partial m_{24}/\partial \upsilon_9 & w_{25} \partial m_{25}/\partial \upsilon_9 \end{bmatrix} \begin{bmatrix} \delta \upsilon_1 \\ \delta \upsilon_2 \\ \vdots \\ \delta \upsilon_8 \\ \delta \upsilon_9 \end{bmatrix}$$

$$\{w_i\} = 0.1 + \left(\frac{R_i - r_m}{r_e - r_m}\right)^2 + \left(\frac{Z_i}{b_g/2}\right)^2 \qquad (i = 1, 2..., p) \qquad (22)$$

Table 2 Basic parameters for the workpiece, standard gear, grinding worm, and dressing disk

Gear Data	
Number of teeth ($\boldsymbol{z_g}$)	19
Normal module ($\boldsymbol{m_n}$)	3.5
Normal pressure angle ($\boldsymbol{\alpha_n}$)	17.5°
Face width ($\boldsymbol{b_g}$)	40mm
Helix angle ($\boldsymbol{\beta_g}$)	35° L.H.
Outside diameter ($\boldsymbol{r_{ag}}$)	88.5315mm
Root diamerter ($\boldsymbol{r_{rg}}$)	72.4315mm
Normal circular tooth thickness ($\boldsymbol{S_n}$)	5.4978mm
Normal coefficient of profile shift ($\boldsymbol{x_n}$)	0
Form diameter	76.2065mm
Grinding Worm Data	
Number of teeth ($\boldsymbol{z_w}$)	3
Outside diameter ($\boldsymbol{r_{aw}}$)	200mm
Lead angle ($\boldsymbol{\lambda_w}$)	3.1472° L.H.
Center distance ($\boldsymbol{E_{wg}}$)	136.2160mm
Crossed angle ($\boldsymbol{\gamma_{wg}}$)	121.8528°
Use area length ($\boldsymbol{b_w}$)	48.1042
Dressing Disk Outside diameter ($\boldsymbol{r_{ad}}$)	123mm
Dressing Disk Center distance ($\boldsymbol{E_{dw}}$)	153.45mm
Dressing Disk Crossed angle ($\boldsymbol{\gamma_{dw}}$)	3.14723°

Table 3 Tooth flank sensitivity topographies for changes in the design variables, $\delta = -0.05$

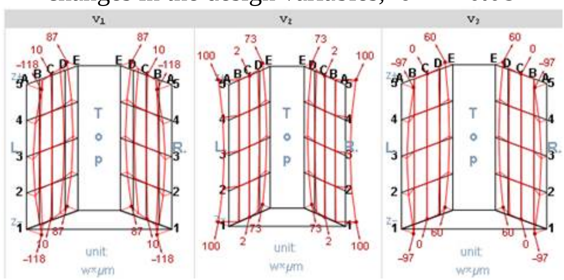

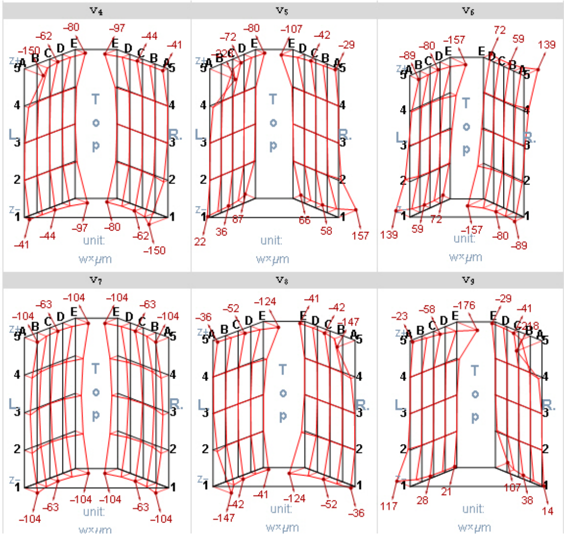

Although the sensitivity matrix $\mathbf{M}_s$ can be calculated using numerical differentiation, because the number of grid points is higher than the number of design variables, the matrix is nonsquare. Hence, changes in the design variables in system Eq. (23) can be solved optimally by using a linear regression technique such as LSE:

$$\{\upsilon_j\} = [\mathbf{IM}_s]\ \{w_i\ m_i\} \qquad (i=1,2...,p;\ j=1,2...,9) \tag{23}$$

To depict the changes in tooth surface topography resulting from design variable modification, we use a numerical example based on the basic workpiece, grinding worm, and dressing disk data listed in Table 2. And Table 3 reports the tooth surface sensitivity topographies δm_i for each modified design variable δv_j. Because the sensitivity matrix is nonsquare and generally ill-conditioned, we avoid numerical divergence by applying SVD to a pseudoinverse of sensitivity matrix M_s, which can be split as follows:

$$[\mathbf{M}_S] = \mathbf{U\,W\,V}^T \tag{24}$$

$$[\mathbf{IM}_S] = \mathbf{V\,W\,U}^T \tag{25}$$

where U and V comprise a unitary matrix, and W is a diagonal eigenvalue matrix with nonnegative real numbers on the diagonal. The design variable changes in system Eq. (25) can be solved using SVD as follows:

$$\{\delta\upsilon_j\} = [IM_s]\{I_i\} \quad (i=1,2,...,p\ ;\ j=1,2...,9) \tag{26}$$

where $\mathbf{W}^+$ is the pseudoinverse of $\mathbf{W}$, which is formed by replacing every nonzero diagonal entry with its reciprocal and transposing the resulting matrix. The modified value $\mathbf{I}_i$ on the mesh grid points of a tooth surface can be expressed as follows, with the superscript representing loop times:

$$I_i^0 = w_i\left(\Omega_{r1}\frac{R_i-r_m}{r_e-r_s} + \Omega_{r2}\left(\frac{R_i-r_m}{r_e-r_s}\right)^2 + \Omega_{z1}\frac{2}{b_g}Z_i + \Omega_{z2}\left(\frac{2}{b_g}Z_i\right)^2\right) \quad (i=1,2...,p) \tag{27}$$

where
Ω_{r1} additional pressure angle
Ω_{r2} profile crowned value
Ω_{z1} lead conical value
Ω_{z2} lead crowned value

By calculating the difference between the calculated and modified tooth surface as input at the next representing loop. The coefficient and total error of the loop can be expressed as shown Fig. 8 to obtain the correct coefficient through the loop operation. The design variable v_i is set at zero in the first trial, and the change in the design variable δv_i is calculated using Eq. (26) with the given residual error topography $\{\delta m_i\}$. The modified design variables $v_i - \delta v_i$ and the corresponding gear generating motions are calculated by substituting $v_i - \delta v_i$ into the polynomials (Eqs. (4), (8), and (20)) to derive the final equation of the machine settings. The aforementioned process can be repeated iteratively until the residual error topography $\{\delta m_i\}$ is within a certain tolerance or remains unchanged.

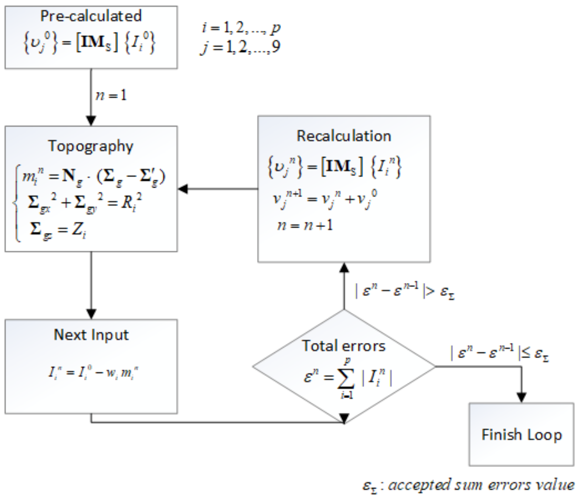

Fig. 8 Convergence loop flow chart

NUMERICAL EXAMPLES

We validate our proposed TDM tooth surface modification method by using three numerical examples, the first two of which involve typical lead double-crowning and conical as the target tooth surface modification but entail using a conventional radial feed method and the TDM method, respectively. In both examples, the twist of the tooth flank is greatly reduced.

The third example, by contrast, has different processes on the left and right tooth surfaces with the modified lead and profile as the target tooth surface modification topology; however, it employs a TDM, which has been shown to be effective for tooth modification.

Example 1

This example uses a 19-tooth, 35° R.H. helical working gear ground by a three-starts grinding worm, whose basic data (working gear, grinding worm, and dressing disk) are listed in Table 3. The target tooth surface modification is shown in Table 6, whose left column lists the normal deviation δm_j at each grid point.

Table 4 Modified values in the profile and lead directions for the workpiece in example 1

tooth	Presure angle	Profile crowned	Lead conical	Lead crowning
	Ω_{r1}	Ω_{r2}	Ω_{z2}	Ω_{z1}
right	0	0.005mm	0.025mm	0
left	0	0.005mm	0.025mm	0

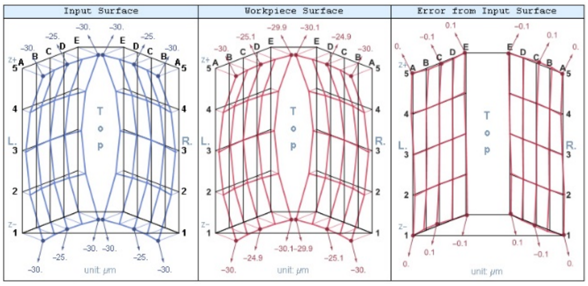

Fig. 9 Tooth surface deviation topography double crowning through TDM

As shown in Fig. 9, the TDM method can be used in a modified double-crowning tooth case. The convergence errors are shown in Fig. 10. This convergence method can markedly reduce the error of the pseudoinverse matrix. As Fig. 9 shows, the modified tooth topology is very close to the target tooth surface. Obviously, the twist on the crowned tooth surface was dramatically reduced.

The simulation results are shown in Figs. 11–14. The profile modified of dressing disk is shown Fig. 11. The tangential dressing feed motion as shown in Fig. 12 and the surface deviation topography of the grinding worm is shown in Fig. 13. The additional gear rotation angle is shown in Fig. 14.

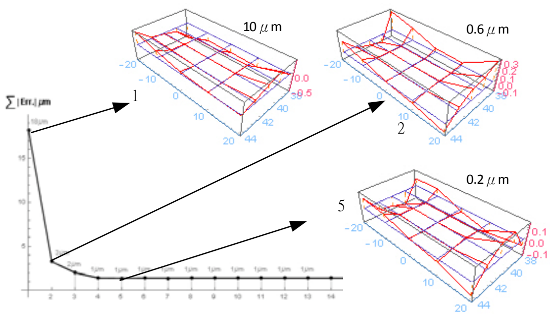

Fig. 10 Total errors in a convergence loop

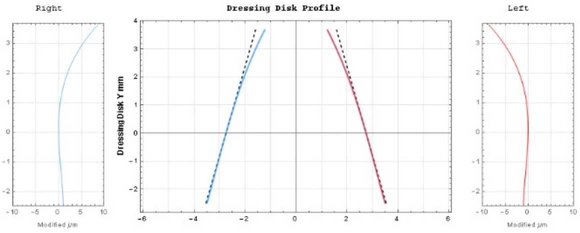

Fig. 11 Modified value of the dressing disk profile

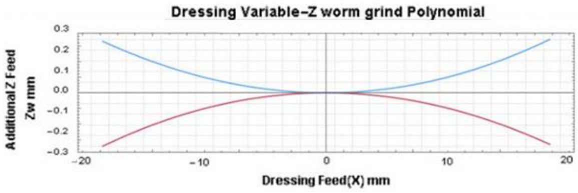

Fig. 12 Tangential feed variables in the dressing process (TDM)

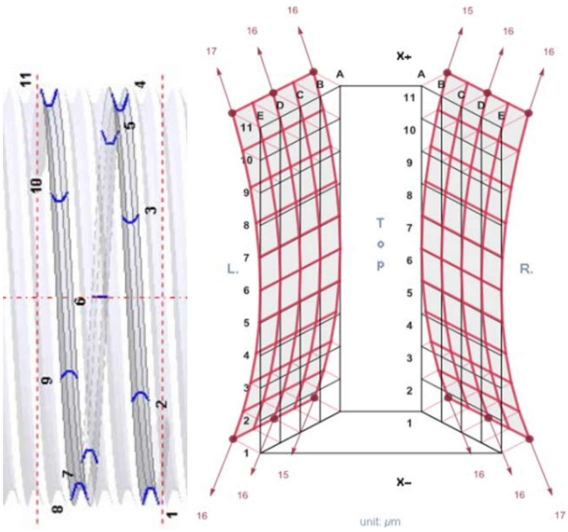

Fig. 13 Surface deviation topography of a grinding worm

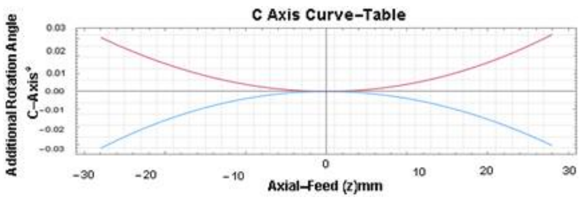

Fig. 14 Additional gear rotation angle feed variables in the grinding process

Example 2

The basic working gear data and target tooth surface modification, shown in Table 5, are the same as those in example 1. However, the tooth surface is modified using the proposed TDM, whose feed variables are solved using SVD (Table 4). We verify the effectiveness of the proposed TDM by using a large conical tooth surface modification. The basic working gear and grinding worm data are the same as those for example 1. The modified value of the tooth surface topology is shown in Fig. 15.

Table 5 Modified values in the profile and lead directions for the workpiece surface in example 2

	Presure angle	Profile crowned	Lead conical	Lead crowning
	Ω_{r1}	Ω_{r2}	Ω_{z2}	Ω_{z1}
right	0	0.005mm	0.050mm	0.100mm
left	0	0.005mm	0.050mm	0.100mm

Again, the tooth surface is modified using the proposed TDM with the design variables solved using SVD. Not only is the modified tooth topology very close to the target tooth surface topology (Fig. 15), but the maximum error of approximately 0.3 μm is negligible. This outcome clearly demonstrates that the proposed TDM is valid for conical tooth surface modification.

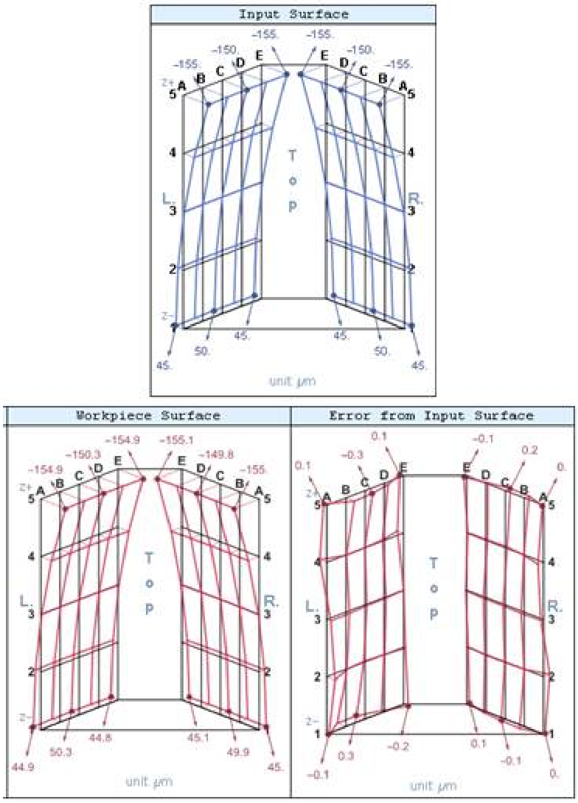

Fig. 15 Tooth surface deviation topography modified by TDM

CONCLUSIONS

Conventionally, the tooth flank of a ground helical gear is crowned by adjusting the radial feed of the grinding worm while the grinding worm is moving axially with respect to the working gear in a modern CNC gear generating grinding machine. However, the tooth flank of a helical gear crowned using this modified radial feed method is frequently twisted when the amount of crowning and the helical angle of the gear are large. Hence, we propose a tooth flank modification method for helical gears that involves using a diagonal (combined tangential and axial) feed combined with gear rotational angle modification in the grinding machine. The used grinding worm is obtained by adjusting the tangential dressing feed of the dressing disk with respect to the grinding worm's rotating angle. Based on our two numerical examples, the proposed TDM method is easily implemented for tooth surface modification in a general CNC gear grinding machine because all the corrective motions are existing CNC controlled axes in modern CNC machines. The proposed TDM method is effective in modifying tooth flanks, even with combined lead, profile, tapered, and pressure angle changes. The flexibility and effectiveness of mitigating twisted tooth flanks are superior to those of the conventional modified radial feed method for tooth crowning.

ACKNOWLEDGMENT

The authors are grateful to the Ministry of Science and Technology, R.O.C., for their grant. Part of this work was performed under Contract No. 104-2622-E-194-014-CC2

REFERENCES

Bouzakis, K. D., and Antoniadis, A., "Optimizing of Tangential Tool Shift in Gear Hobbing," *CIRP Ann. Manuf. Technol.*, Vol. 44, No. 1, pp. 75-78 (1995).

Chen, K.-H., Chen, C.-J., and Fong, Z.-H., "Computer Simulation for the Cutting Process of a CNC Hobbing Machine," *Chinese Society of Mechanism and Machine Theory Conference*, Chiayi, Taiwan, pp. 154-161 (2009).

Dudley, D. W., *Dudley's Gear Handbook: The Design, Manufacture, and Application of Gears*, 2nd ed., McGraw-Hill, New York (2011).

Fan, Q., DaFoe, R. S., and Swanger, J. W., "Higher-Order Tooth Flank Form Error Correction for Face-Milled Spiral Bevel and Hypoid Gears," *ASME J. Mech. Des.*, Vol. 130, No. 7, pp. 072601 (2008).

Hsu, R.-H., and Tsay, C.-B., "Study on the Anti-Twist Helical Gear Tooth Flank with Longitudinal Tooth Crowning," *ASME J. Mech. Des.*, Vol. 136, No. 6, pp. 061007 (2014).

Hsu, R.-H., and Su, H., "Tooth Contact Analysis for Helical Gear Pairs Generated by a Modified Hob with Variable Tooth Thickness," *Mech. Mach. Theory*, Vol. 71, pp. 40-51 (2014).

Jiang, J., and Fang, Z., "High-Order Tooth Flank Correction for a Helical Gear on a Six-Axis CNC Hob Machine," *Mech. Mach. Theory*, Vol. 91, pp. 227-237 (2015).

Karpuschewski, B., Knoche, H.-J., and Hipke, M., "Gear Finishing by Abrasive Processes," *CIRP Ann.: Man. Tech.*, Vol. 57, No. 2, pp.

621-640. (2008).

Litvin, F. L., Zhang, J., and Handschuh, R. F., “Crowned Spur Gears: Methods for Generation and Tooth Contact Analysis - Part 2: Generation of the Pinion Tooth Surface by a Surface of Revolution,” *ASME J. Mech. Des.*, Vol. 110, No. 3, pp. 343-347 (1988).

Litvin, F. L., and Fuentes, A., *Gear Geometry and Applied Theory*, 2nd ed., Cambridge University Press, Cambridge, UK (2004).

Lange, J., “How Are You Dealing with the Bias Error in Your Helical Gears,” *AGMA Fall Technical Meeting*, Indianapolis (2009).

Siemens, *Sinumerik 840D sI/828D Operator’s Manual* (2012).

Lange, J., “How Are You Dealing with the Bias Error in Your Helical Gears,” *AGMA Fall Technical Meeting*, Indianapolis (2009).

Shih, Y.-P., and Chen, S.-D., “A Flank Correction Methodology for a Five-Axis CNC Gear Profile Grinding Machine,” *Mech. Mach. Theory*, Vol. 47, pp. 31-45 (2012).

Shih Y.-P. and Chen S.-D., “Free-Form Flank Correction in Helical Gear Grinding Using a Five-Axis Computer Numerical Control Gear Profile Grinding Machine,” *J. Manuf. Sci. Eng.*, Vol. 134, No. 4, pp. 41006 (2012).

Tran, V.-T., Hsu, R.-H., and Tsay, C.-B., “A Novel Finish Hobbing Methodology for Longitudinal Crowning of a Helical Gear With Twist-Free Tooth Flanks by Using Dual-lead Hob Cutters,” *ASME Paper* No. IMECE2014-36149, pp. 1-9 (2014).

Winkel, O., “New Developments in Gear Hobbing,” *Gear Tech.*, March/April, pp. 47-55 (2010).

Xu, H., Chakraborty, J., and Wang, J. C., “Effects of Axle Deflection and Tooth Flank Modification on Hypoid Gear Stress Distribution and Contact Fatigue Life,” *AGMA Fall Technical Meeting*, 05FTM09, Detroit, MI (2009).

NOMENCLATURE

α_n normal pressure angle
b_w face width of grinding worm
b_g face width of gear
β_g helical angle of gear
δm change in the normal deviation
δv_j change value of design variables
E_{dw} center distance between dressing disk and grinding worm
E_{gw} center distance between grinding worm and workpiece
F_T tangential feed when grinding
F_R radial feed when grinding
γ_{dw} cross angle between dressing disk and grinding worm
γ_{gw} cross angle between grinding worm and workpiece
λ_w lead angle of standard grinding worm
m_n normal module
m_w gear ratio of grinding worm and workpiece
p The total number of mesh grid points
P_w screw parameter of the standard grinding worm
ϕ_A The actual crossed angle between grinding worm and workpiece
ϕ_B the rotating angle of grinding worm
ϕ_C the rotating angle of workpiece
ϕ_w rotation angle of grinding worm
r_e End of active profile (EAP)
r_m the center of tooth profile
r_{pd} pitch radius of dressing disk
r_{pw} pitch circle radius of grinding worm
r_{pg} pitch circle radius of gear
r_s Start of active profile (SAP)
s line parameter of dressing disk
s_n tooth thickness of the gear normal surface
θ angle parameter of dressing disk
u_{dt} tangential feed parameter
u_{dz} axial feed parameter
U comprise a unitary matrix of SVD
V comprise a unitary matrix of SVD
v_i i=1 ~3, i order coefficient of dressing disk profile parameter
i=4~5, (i-2) order coefficient of dressing variable lead parameter
i=6~9 , constant of grinding crossed angle , radial feed design , 2nd and 3rd rotation angle parameter
W diagonal eigenvalue matrix of SVD
x_{ng} profile shift of the gear
z axial feed parameter
z_w Thread number of grinding worm
z_g Tooth number of gear
z_i topography grid mesh points in face width direction

在創成齒輪磨床中利用切向運動修整螺旋齒輪齒面

陳冠宏　　馮展華
國立中正大學機械工程學系

摘 要

在創成磨齒加工螺旋齒輪的齒面時，為了進行齒面隆齒修整，通常在蝸桿型式砂輪軸向進給時透過同動徑向位移來形成修整動作。然而，徑向進給的隆齒方法會造成螺旋齒輪的齒面扭曲。因

此，我們提出了一種螺旋齒輪齒面隆齒修形方法，運用蝸桿砂輪的對角進給，亦即蝸感式砂輪進行加工齒輪的切向和軸向聯合進給來修整齒輪齒面(TDM)。同時計算砂輪修砂時，運用附加的切向修整運動(TDM)所需要的修砂輪廓。由於所提出的TDM 方法需要運動都是現代齒輪磨床中現有的電腦數控軸，因此所提出的方法能無需修改齒輪磨齒機的硬體設備來實現。本文以兩個數值範例驗證磨齒加工螺旋齒輪時所提出的具有四個同時控制軸的 TDM 齒面修整方法，來達到齒輪齒面隆齒修整時避免齒面扭轉產生。